Nimesulide inhibits tumor growth in mice implanted hepatoma: overexpression of Bax over Bcl-2[1]

LI Xiao-Hong, LI Jun-Jie[2], ZHANG Hai-Wei[3], SUN Peng, ZHANG Yan-Ling, CAI Shao-Hui, REN Xian-Da[4]

Department of Pharmacokinetics, Pharmacy College, [2]Department of Clinical Pharmacology, Huaqiao Affiliated Hospital, [3]Department of Pathology, Medical College, Ji-nan University, Guangzhou 510632, China

ABSTRACT

AIM: To investigate whether nimesulide could suppress tumor growth and induce apoptosis in implanted hepatoma mice and to explore the molecular mechanisms. **METHODS:** Male mice received nimesulide 10 mg/kg, 20 mg/kg, and 40 mg/kg ig daily for 21 d. Electron microscopy (EM), flow cytometry (FCM), DNA ladder, radioimmunoassay (RIA), and Western blot analysis were employed to investigate effect of nimesulide on mice hepatoma and the related molecular mechanisms. **RESULTS:** Nimesulide inhibited the growth of hepatoma (from 14 % to 62 %) and elicited typical apoptotic morphologic changes. The DNA ladder of high dose nimesulide was more clearly observed and apoptotic rate was 51.3 %±1.5 %. Nimesulide also decreased cyclooxygenase-2 (COX-2), prostaglandin E_2 (PGE_2) and Bcl-2 expression, while increased the level of Bax protein. **CONCLUSION:** Nimesulide suppresses tumor growth and induces apoptosis by inhibiting COX-2 and PGE_2 expression, which may be related to overexpression of Bax over Bcl-2.

INTRODUCTION

Cyclooxygenase (COX) is responsible for the conversions of arachidonic acid to prostaglandin (PG). Increased PGE_2 synthesis occurs in adenomatous polyps, colonic carcinomas[1], and epithelial ovarian cancers[2]. Significant advances have furthered our understanding of the potential role of PG in cancer biology. Evidences from *in vitro* and *in vivo* studies suggest an important role for PG and their synthesizing enzyme COX-2 in carcinogenesis[1,3]. In mammalian cells, the COX enzyme consists of two isozymes encoded by separate genes. The COX-1 gene is constitutively expressed in most tissues, and the protein levels do not fluctuate in response to stimuli such as cytokines or growth factors[4]. The COX-2 gene has been characterized as an immediate early gene associated with cellular growth and differentiation. Recently, elevated levels of COX-2 expression have been found in human carcinomas, including examples in the colon, lung, stomach, and pancreas[3,5-7]. Recent studies have suggested that overexpression of COX-2 might be one of the leading factors in hepatic carcinogenesis[8]. COX-2 can induce angiogenesis via vascular endothelial growth factor (VEGF) and prostaglandin production and can also inhibit apoptosis by inducing the antiapoptotic factor Bcl-2 as well as activating antiapoptotic signalling through Akt/PKB[9]. Therefore, the use of selective inhibitors for the down-regulation of COX-2 activity might be a

target for preventing hepatic carcinoma development. Our previous studies have demonstrated that selective COX-2 inhibitors, SC58125 and JTE-522 have exerted cell proliferation inhibition and apoptosis induction on some cancer cell lines *in vitro*[10,11]. Nimesulide, a sulfonanilide class COX-2 inhibitor which can bind to the large catalytic moiety of COX-2 but not COX-1, preferentially inhibits sheep placenta COX-2 activity *in vitro*, with an IC_{50} of 0.07 μmol/L and appears to possess much less adverse on the gastrointestinal tract than non-specific NSAID[12,13]. Studies indicated that nimesulide possessed chemopreventive activity against intestinal polyp development in mice[12], PhIP-induced mammary carcinogenesis and CDAA-induced hepatocarcinogenesis in rats[14-16]. Some effort to assess the efficacy of nimesulide as a anticancer agent compared to other potential anticancer compounds, including conventional NSAID and other selective COX-2 inhibitors for liver cancer, in experimental animal models seems worthwhile. So, the present study was designed to determine the effects of nimesulide on hepatoma *in vivo*.

MATERIALS AND METHODS

Materials Nimesulide was purchased from Sigma Chemical Co (St Louis, MO, USA) and suspended in phosphate-buffered saline (PBS) pH 7.2 solutions. Monoclonal anti-mouse antibodies of COX-2, Bcl-2, Bax, C-myc, and β-actin were obtained from Santa Cruz. Final dilutions were 1:300 for bcl-2 and bax antibodies, 1:100 for anti-c-myc antibodies, 1:500 for COX-2 and β-actin antibodies. RIA kit was purchased from Institute of Blood, Suzhou Medical University, China.

Animals and tumor model Male Kunming mice weighing 18-22 g were sterilely inoculated subcutaneously in the flank with 1×10^7 mice hepatoma cell line H22 and were bred on standard mouse chow and water freely under standard conditions. They were randomly separated into four groups (10 mice in each group). The following day they were treated with nimesulide 10 mg/kg, 20 mg/kg, and 40 mg/kg, or vehicle, respectively and were ig per day from d 1 to d 21. Throughout the experimentation period, food and water was available to animals *ad libitum*. After 21-d test period animals were killed by cervical dislocation. Solid tumor was weighed, then fixed or pulverized using a mortar and pestle.

Tumor inhibition rate Tumor growth was evaluated by the inhibition rate as assessed by the formula: IR=(1-T/C)×100 %. Where IR is the mean inhibition rate, T is the mean tumor weight in the treatment group and C is the mean tumor weight in the control group.

Morphological analysis of apoptosis Morphological changes in the nuclear chromatin of cells undergoing apoptosis were detected by electron microscopy (EM). Solid tumors were fixed with glutaraldehyde 20 mL/L. EM analysis was performed as described previously[17]. Thin sections were viewed in an electron microscope (JEM-100CX 11/T, Japan).

DNA ladder detection Assay pulverized solids were lysed and cells were harvested and rinsed twice in ice-cold PBS. The final pellet was lysed in 0.3 mL Tris-HCl buffer 10 mmol/L (pH 7.4) containing edetic acid 25 mmol/L, 0.5 % SDS, and proteinase K 0.1 g/L (Sigma) at 37 ℃ for 12 h. DNA was extracted with an equal volume of phenol/chloroform/isoamyl alcohol (25:24:1) and precipitated with 2 volumes of ice-cold absolute ethanol and 1/10 volume sodium acetate 3 mol/L. DNA was collected, washed once with 70 % ethanol, and dissolved in TE buffer (Tris-HCl 10 mmol/L and edetic acid 1 mmol/L, pH 8.0). Then, the isolated DNA samples were incubated with RNase I 10 g/L for 1 h at 37 ℃. An equal amount (10 mg/well) of DNA was electrophoresed in 1.5 % agarose gel impregnated with ethidium bromide (0.1 g/L) for 2 h at 60 V. DNA markers were run at the same time. DNA fragments were visualized by ultraviolet light.

Flow cytometry Cell suspension was fixed in ice-cold 70 % ethanol in PBS, and stored at -20 ℃. Prior to analysis, the cells were washed and resuspended in PBS and incubated with RNase I 1 g/L and propidium iodide 20 g/L at 37 ℃ for 30 min. The analysis of samples was performed by a flow cytometer (Coulter EPICS XL).

Radioimmunoassay (RIA) The amounts of immunoreactive PGE_2 in samples of solid tumor were determined by RIA using a commercially available RIA kit according to the manufacturer's instructions. Briefly, to each polypropylene RIA tube were added 100 μL of anti-PGE_2, ^{125}I-PGE_2, and PGE_2 or the sample. Immune complexes were precipitated 24 h later with 1 mL of polyethylene glycol solution, and the radioactivity in the precipitate was determined by a gamma counter. There was no nonspecific interference of the assay by the components of the sample. Determinations were carried out in triplicate and the mean and standard

deviations were obtained.

Western blot analysis of c-myc, COX-2, Bax and Bcl-2 Cells were lysed in Tris-HCl buffer 50 mmol/L (pH 7.2) containing sodium chloride 0.137 mol/L, 1 % Brij 96, 4-(2-aminoethyl)-benzenesulphonyl fluoride (AEBSF) 0.2 mmol/L, edetic acid 1 mmol/L, leupeptin 20 μmol/L, and pepstatin 1 μmol/L (all Sigma). Cell lysates were centrifuged at 15 000×*g* for 5 min at 4 ℃. The resulting solution was centrifuged for 15 min as above. Protein concentration was determined using a Bio-Rad DC kit (BioRad, Hemel Hempstead, UK). SDS-PAGE was performed using 100 μg total protein aliquots together with pre-stained molecular weight standards. Proteins were transferred to polyvinylidene fluoride membranes which were then blocked with dried skimmed milk powder in Tween Tris-buffered saline (TTBS) for 2 h at 20 ℃. Membranes were probed with primary antibodies in TTBS for 2 h at 20 ℃. Horseradish peroxidase-conjugated secondary antibodies were incubated with proteins in the second reaction for 2 h at 20 ℃. Immunoreactive protein was detected using ECL chemiluminescence.

Statistical analysis Results were expressed as mean±SD. Statistical analysis of the results was performed using two-tailed Student's *t*-test. $P<0.05$ was considered statistically significant.

RESULTS

Tumor inhibition rate Administration ig of nimesulide suppressed tumor growth in a dose-dependent manner. The 1st maximum inhibition rate was 62 % and the 2nd one was 61 % for the high dose group. This experiment was repeated twice (Tab 1).

Electron microscopy assay The morphologic characteristics of apoptosis were clearly observed under EM after treatment with nimesulide. Control group (Fig 1A) showed even distribution of chromatin and a normal nucleolus. Upon nimesulide treatment in hepatoma mice, two apoptotic cells illustrated ultrastructural changes of apoptosis (Fig 1B). Cells shrinkaged and the nucleus showed deep condensation that was revealed by the appearance of a large gap around the nucleus. The condensed chromatin showed large sharply marginated electron dense masses that abutted on the nuclear envelope. These results identified that the hepatoma cell underwent apoptosis.

DNA ladder detection assay Agarose gel electrophoresis exhibited DNA ladder formation in hepatoma

Tab 1. Tumor weight and inhibition rate of mice implanted hepatoma treated with nimesulide. n=10. Mean±SD. $^c P< 0.01$ *vs* control. $^e P<0.05$, $^f P<0.01$ *vs* nimesulide 20 mg/kg.

Group	Dose/ mg·kg⁻¹	X1	R1/%	X2	R2/%
Control	-	3.67±1.7	-	3.69±1.6	-
Nimesulide	10	3.14±1.2^f	14	3.11±1.4^f	16
	20	2.59±0.9^c	30	2.56±0.9^c	31
	40	1.38±0.8^{ce}	62	1.43±0.7^{ce}	61

X1: the first mean tumor weight; R1: the first mean inhibition rate; X2: the second mean tumor weight; R2: the second mean inhibition rate.
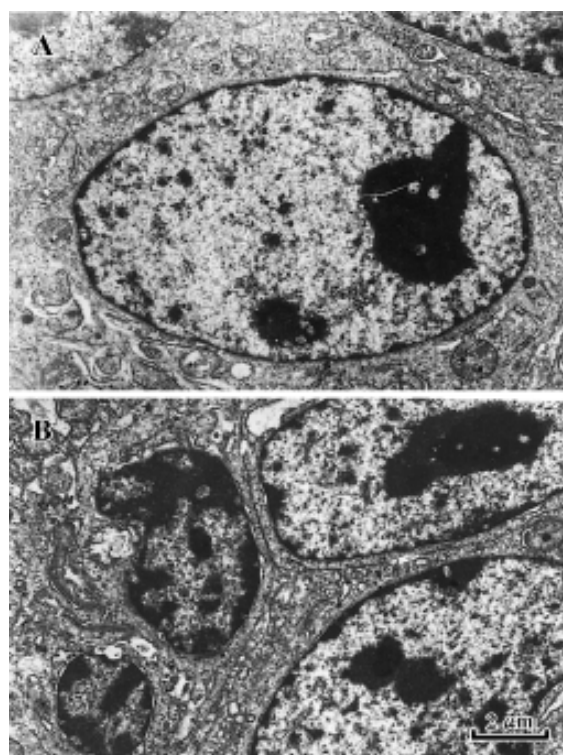
Fig 1. Electron microscope images of untreated control (A) and nimesulide 40 mg/kg-treated (B) mice hepatoma. ×5000.

after 3-week treatment with nimesulide at doses from 10 mg/kg to 40 mg/kg. Nimesulide was found to significantly induce DNA fragmentation in a dose-dependent manner (Fig 2).

Flow cytometry Apoptotic damage of DNA was detected according to the Sub-G1 peak on a flow cytometer. The apoptotic cells can be observed on a DNA histogram as a subdiploid or 'pre-G1' peak. Obviously, a sub-G1 peak and the apoptotic index was
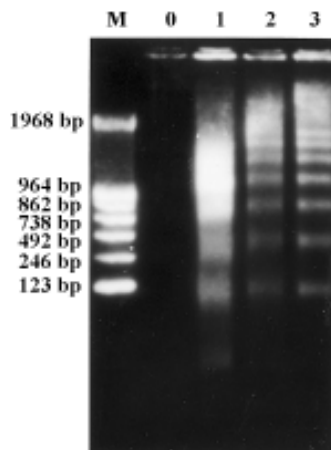
Fig 2. DNA ladder pattern formation of mice hepatoma. The formation of oligonucleosomal fragments was determined by 1.5 % agarose gel electrophoresis. M: DNA markers; lanes 0-3: control, nimesulide 10 mg/kg, 20 mg/kg, and 40 mg/kg.

increased from 3.0 %±1.0 % to 51.3 %±1.5 % after nimesulide treatment in a dose-dependent manner (Tab 2).

Tab 2. Effect of nimesulide-induced apoptosis in mice hepatoma. Apoptotic index was determined by FCM analysis. *n*=3. Mean±SD. $^c P<0.01$ *vs* control. $^e P<0.05$, $^f P<0.01$ *vs* nimesulide 20 mg/kg.

Group	Dose/mg·kg^{-1}	Apoptotic index/%
Control	-	3.0±1.0
Nimesulide	10	15.3±0.6^{cf}
	20	41.7±3.8^c
	40	51.3±1.5^{ce}

The effect of nimesulide on PGE$_2$ production by RIA The increased dose of nimesulide treatment was accompanied with a reduction in PGE$_2$ production in mice hepatoma. The dose-dependent decrease in PGE$_2$ production reached the lowest after treatment with nimesulide 40 mg/kg ($P<0.01$, Fig 3).

Western blot analysis of c-myc, COX-2, Bax, and Bcl-2 To further elucidate the mechanisms of nimesulide-induced apoptosis in mice hepatoma, we evaluated the Bcl-2 family proteins, c-myc protein, and COX-2 in the apoptotic process by Western blot analysis. After nimesulide treatment Bax protein level was significantly increased. However, Bcl-2 and COX-2 pro-
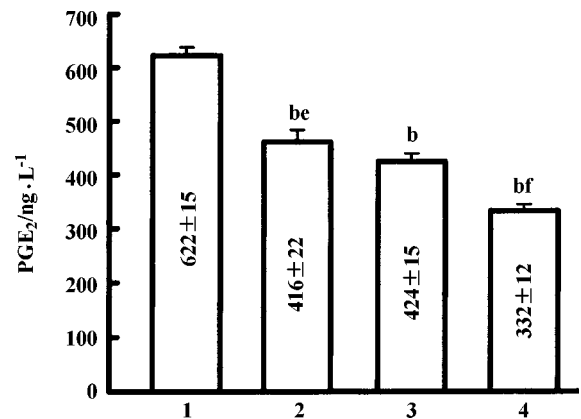
Fig 3. Effect of nimesulide on PGE$_2$ production in mice hepatoma. Column 1-4: control, nimesulide 10 mg/kg, 20 mg/kg, and 40 mg/kg. *n*=3. Mean±SD. $^b P<0.05$ *vs* control; $^e P<0.05$, $^f P<0.01$ *vs* nimesulide 20 mg/kg.

tein levels were greatly decreased. No change was detected on c-myc expression. The expressions of Bax, Bcl-2, and COX-2 were regulated in a dose-dependent manner (Fig 4).
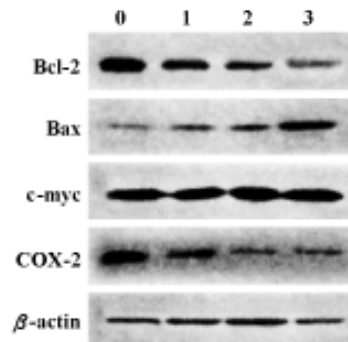
Fig 4. Effect of nimesulide on expression of Bcl-2, Bax, c-myc, and COX-2 in mice hepatoma. 0: control; 1-3: nimesulide 10 mg/kg, 20 mg/kg, and 40 mg/kg. β-actin was used as an internal control.

DISCUSSION

In the present study, we demonstrated a clear tumor inhibition and apoptosis induction of nimesulide against mice implanted hepatoma. In addition, nimesulide did not cause any toxic lesions or side effects such as gastrointerstinal bleeding in this experiment.

It is conceivable that high concentrations of PGE$_2$ result from up-regulation of COX-2. These cellular events might result in uncontrolled cellular proliferation, reduced apoptosis, or both, which contributes to the emergence of the neoplastic phenotype. As demon-

strated in the present study, nimesulide inhibited COX-2 and PGE$_2$ expression in a dose-dependent manner, indicating that COX-2 and/or PGE$_2$ play a pivotal role in mice implanted hepatoma. So it is very important to completely elucidate the involved molecular pathways for its anti-tumor activity.

Souto *et al*[18] suggests Kupffer cell-derived prostanoids may regulate Bcl-2 expression in the hepatocyte. Hepatic Bcl-2 protein expression was four fold lower in the livers from nimesulide-treated CVF rats. Alteration of Bcl-2 family proteins is complex but important in cancer. Overexpression of COX-2 in a rat intestinal epithelial cell line was previously reported to be associated with induction of Bcl-2 and prevention of apoptosis[19]. The ability of reduced levels of Bcl-2 protein to block apoptosis induced by most cytotoxic agents defines a new multidrug resistance mechanism[20-23]. Bax, a homologue of Bcl-2, which forms heterodimers with Bcl-2, blocks the action of Bcl-2 and thus acts as a promoter of apoptosis. When Bax predominates, programmed cell death is accelerated and the death repressor activity of Bcl-2 is counted. Previous studies have shown that alterations in the ratio between proapoptotic and antiapoptotic members of the Bcl-2 family, rather than the absolute expression level of any single Bcl-2 family member, can determine apoptotic sensitivity. Therefore, it appears to be the relative ratios of Bax and Bcl-2 that determine the fate of a cell, rather than the absolute concentrations of either. In this study, we found that both Bcl-2 and Bax were expressed in mice hepatoma, and nimesulide induced Bax expression and reduced Bcl-2 expression. This may imply that nimesulide-induced apoptosis in mice hepatoma is regulated via preferential overexpression of Bax over Bcl-2. The effects were more obvious following the enhancement of nimesulide dose.

C-myc acts on a common pathway affecting cell death, and is the upstream of Bcl-2. However, no change in C-myc expression was detected in our study. It may suggest that nimesulide induced apoptosis appeared to be C-myc-independent.

In conclusion, nimesulide leads to a marked growth inhibition of mice hepatoma, based on the induction of apoptosis which may be related to overexpression of Bax over Bcl-2, and thus may offer therapeutic potential in human hepatocarcinogenesis.

REFFRENCES

1 Pugh S, Thomas G. Patients with adenomatous polyps and cancinomas have increased colonic mucosal prostaglandin E2. Gut 1994; 35: 675-8.

2 Munkarah AR, Morris R, Baumann P. Effects of prostaglandin E2 on proliferation and apoptosis of epithelial ovarian cancer cells. J Soc Gynecol Investig 2002; 9: 168-73.

3 Wolff H, Saukkonen K, Anttila S, Karjalanainen A, Vainio H, Ristimaki A. Expression of COX-2 in human lung carcinoma. Cancer Res 1998; 58: 4497-501.

4 Vane J. Towards a better aspirin. Nature 1994; 367: 215-6.

5 Sheng H, Shao J, Kirkland S. Inhibition of human coloncancer cell growth by selective inhibition of cyclooxygenase-2. J Clin Invest 1997; 99: 2254-9.

6 Murata H, Kawano S, Tsuji S. Cyclooxygenase-2 overexpression enhances lymphatic invasion and metastasis in human gastric carcinoma. Am J Gastroenterol 1999; 94: 451-5.

7 Molina MA, Sitja AM, Lemoine MG. Increased COX-2 expression in human pancreatic carcinomas and cell lines: growth inhibition by NSAIDs. Cancer Res 1999; 59: 43-56.

8 Koga H, Sakisaka S, Ohishi M. Expression of cyclooxygenase-2 in human hepatocellular carcinoma: relevance to tumor dedifferentiation. Hepatology 1999; 29: 688-90.

9 Arico S, Pattingre S, Bauvy C, Gane P, Barbat A, Codogno P, *et al.* Celecoxib induces apoptosis by inhibiting 3-phosphoinositide-dependent protein kinase-1 activity in the human colon cancer HT-29 cell line. J Biol Chem 2002; 277: 27613-21.

10 Ke XL, Li HL, Chen DD, Ren XD, Zhang HW, Chen XD, e*t al*. Changes in NF-kB, AP-1 and caspase-3 on apoptosis induced by SC-58125 in HepG2 human hepatocarcinoma cells. Chin J Pathophysiol 2001; 17: 1188-92.

11 Li HL, Chen DD, Zhang HW, Zhong L, Ren XD. JTE-522, a selective COX-2 inhibitor, inhibits cell proliferation and induces apoptosis in human endometrial cancer line RL95-2 cells. Acta Pharmacol Sin 2002; 23: 631-7.

12 Taketo MM. Cyclooxygenase-2 inhibitors in tumorigenesis (Part I). J Natl Cancer Inst 1998; 90: 1529-36.

13 Tavares IA, Bishai PM, Bennett. Activity of nimesulide on constitutive and inducible cyclooxygenases. Arzneimittelforschung 1995; 45: 1093-5.

14 Seiichi N, Masato F, Mami T. Suppression of intestinal polyp development by nimesulide, a selective cyclooxygenase-2 inhibitor, in Min mice. Jpn J Cancer Res 1997; 88: 1117-20.

15 Seijchi N, Toshihisa O, Toshihiko K. Chemoprevention by nimesulide, a selective cyclooxygenase-2 inhibitor, of 2-amino-1-methyl-6-phenylimidazo [4,5-b] pyridine (PhIP)-induced mammary gland carcinogenesis in rats. Jpn J Cancer Res 2000; 91: 886-92.

16 Ayumi D, Wakashi K, Akiko M. Increased expression of cyclooxygenase-2 protein during rat hepatocarcinogenesis caused by a choline-deficient, *L*-amino acid-defined diet and chemopreventive efficacy of a specific inhibitor, nimesulide. Carcinogenesis 2002; 23: 245-56.

17 Peng LM, Liu JJ. A novel method for quantitative analysis of apoptosis. Lab Invest 1997; 77: 547-55.

18 Souto EO, Miyoshi H, Dubois RN. Kupffer cell-derived cyclooxygenase-2 regulates hepatocyte Bcl-2 expression in

choledocho-venous fistula rats. Am J Physiol Gastrointest Liver Physiol 2001; 280: 805-11.

19 Tsujii M, DuBois RN. Alterations in cellular adhesion and apoptosis in epithelial cells over expressing prostaglandin endoperoxide synthase 2. Cell 1995; 83: 493-501.

20 Xiao D, Gu Z, Zhu SP. Quercetin down-regulated Bcl-2 gene expression in human leukemia HL-60 cells. Acta Pharmacol Sin 1998; 19: 551-3.

21 Zhu XF, Zhang XS, Li ZM, Yao YQ, Xie BF, Zeng YX, *et al.* Apoptosis induced by ceramide in hepatocellular carcinoma Bel7402 cells. Acta Pharmacol Sin 2000; 21: 225-8.

22 Leng Y, Feng Y, Cao L, Gu ZP. Effects of droloxifene on apoptosis and Bax, Bcl-2 protein expression of luteal cells in pseudopregnant rats. Acta Pharmacol Sin 2001; 22: 155-62.

23 Leng Y, Feng Y, Cao L, Gu ZP. Apoptosis induced by droloxifene and Bax, Bcl-2 protein expression of luteal cells in pseudopregnant rats. Acta Pharmacol Sin 2001; 22: 327-34.